Solid-state Structures of Platinum–Sulphur–Nitrogen Stacking Compounds: $[Pt(S_2N_2)(PMe_2Ph)_2]$, $[Pt(S_2N_2H)(PMe_2Ph)_2]Cl$, $[Pt(S_2N_2H)(PMe_2Ph)_2]PF_6$, and $[Pd(S_2N_2H)(PMe_2Ph)_2]BF_4$†

Ray Jones, Paul F. Kelly, David J. Williams,* and J. Derek Woollins
Department of Chemistry, Imperial College of Science and Technology, South Kensington, London SW7 2AY

The *X*-ray crystal structures of $[Pt(S_2N_2)(PMe_2Ph)_2]$, $[Pt(S_2N_2H)(PMe_2Ph)_2]Cl$, $[Pt(S_2N_2H)(PMe_2Ph)_2]PF_6$, and $[Pd(S_2N_2H)(PMe_2Ph)_2]BF_4$ are reported. The effect of protonation of the $S_2N_2^{2-}$ ligand and the requirements for stacking are discussed.

In a preliminary communication[1] we reported on the preparation of mixed-ligand metal–sulphur–nitrogen–phosphine complexes which, contrary to the then prevailing opinion, stack in the solid state. This work is part of a wider study on the use of transition-metal centres in the stabilisation of reactive S–N fragments[2-6] such as $(Me_3Si)NSN^-$, S_3N^-, $S_2N_2^{2-}$, or $S_2N_2H^-$ and we have recently reviewed this topic.[7] Here we report and discuss in detail the structures of representative $[Pt(S_2N_2)(PR_3)_2]$ and $[M(S_2N_2H)(PR_3)_2]X$ complexes. Previously only scattered reports have been available and this is the first detailed, systematic study of these systems.

Experimental

The complexes were prepared as described previously.[8,9] The n.m.r. and i.r. spectra have been detailed in previous reports.[8,9] Crystals suitable for *X*-ray analysis were obtained by slow diffusion of hexane into dichloromethane or chloroform solutions.

Crystal Data.—Complex $[Pt(S_2N_2)(PMe_2Ph)_2]$ (**1**). $C_{16}H_{22}N_2P_2PtS_2$, $M = 563.51$, monoclinic, $a = 17.111(6)$, $b = 13.742(7)$, $c = 17.924(7)$ Å, $\beta = 109.52(3)°$, $U = 3\,986(3)$ Å^3, space group $C2/c$, $Z = 8$, $D_c = 1.88$ g cm^{-3}. Yellow air-stable prisms, crystal dimensions $0.2 \times 0.1 \times 0.1$ mm, μ(Cu-K_α) = 168.0 cm^{-1}, $\bar{\lambda} = 1.541\,78$ Å, $F(000) = 2\,175$.

Complex $[Pt(S_2N_2H)(PMe_2Ph)_2]Cl$ (**2**). $C_{16}H_{23}ClN_2P_2PtS_2 \cdot 0.5CH_2Cl_2$, $M = 642.44$,‡ monoclinic, $a = 9.710(4)$, $b = 25.871(11)$, $c = 9.805(4)$ Å, $\beta = 90.62(3)°$, $U = 2\,463(2)$ Å^3, space group $P2_1/c$, $Z = 4$, $D_c = 1.74$ g cm^{-3}. Green air-stable prisms, crystal dimensions $0.3 \times 0.1 \times 0.2$ mm, μ(Cu-K_α) = 157.0 cm^{-1}, $\bar{\lambda} = 1.541\,78$ Å, $F(000) = 1\,244$.‡

Complex $[Pt(S_2N_2H)(PMe_2Ph)_2]PF_6$ (**4**). $C_{16}H_{23}F_6N_2P_3PtS_2$, $M = 709.49$, monoclinic, $a = 8.853(2)$, $b = 17.162(5)$, $c = 14.403(8)$ Å, $\beta = 104.06(3)°$, $U = 2\,418(1)$ Å^3, space group $P2_1/c$, $Z = 4$, $D_c = 1.96$ g cm^{-3}. Green air-stable plates, crystal dimensions $0.2 \times 0.1 \times 0.1$ mm, μ(Cu-K_α) = 150.1 cm^{-1}, $\bar{\lambda} = 1.541\,78$ Å, $F(000) = 1\,368$.

Complex $[Pd(S_2N_2H)(PMe_2Ph)_2]BF_4$ (**5**). $C_{16}H_{23}BF_4N_2P_2PdS_2$, $M = 562.44$, monoclinic, $a = 8.584(1)$, $b = 17.158(3)$, $c = 16.155(3)$ Å, $\beta = 104.93(1)°$, $U = 2\,299(1)$ Å^3, space group $P2_1/n$, $Z = 4$, $D_c = 1.63$ g cm^{-3}. Olive green air-stable prisms, crystal dimensions $0.5 \times 0.5 \times 0.3$ mm, μ(Cu-K_α) = 100.5 cm^{-1}, $\bar{\lambda} = 1.541\,78$ Å, $F(000) = 1\,128$.

† [Di(azathienyl)-S^1,N^4]bis(dimethylphenylphosphine)platinum(II), [di(azathien)-1-yl-S^1,N^4]bis(dimethylphenylphosphine)platinum(II) chloride and hexafluorophosphate, and [di(azathien)-1-yl-S^1,N^4]bis-(dimethylphenylphosphine)palladium(II) tetrafluoroborate respectively.

Supplementary data available: see Instructions for Authors, *J. Chem. Soc., Dalton Trans.*, 1988, Issue 1, pp. xvii—xx.

‡ Includes a contribution from a disordered solvent fragment, refined as $0.5CH_2Cl_2$.

Table 1. Atomic co-ordinates ($\times 10^4$) for $[Pt(S_2N_2)(PMe_2Ph)_2]$ (**1**)

Atom	*x*	*y*	*z*
Pt	3 774(1)	−1 482(1)	−354(1)
S(1)	4 004(3)	−1 369(4)	1 404(3)
S(2)	3 596(3)	−48(3)	197(3)
P(1)	3 946(2)	−2 999(3)	−777(2)
P(2)	3 560(2)	−774(2)	−1 547(2)
N(1)	3 990(6)	−2 054(7)	772(4)
N(2)	3 716(8)	−248(9)	1 085(7)
C(1)	4 946(7)	−3 182(9)	−892(7)
C(2)	5 567(7)	−2 508(11)	−585(7)
C(3)	6 317(8)	−2 609(13)	−676(8)
C(4)	6 486(11)	−3 427(17)	−1 060(13)
C(5)	5 875(12)	−4 101(15)	−1 372(11)
C(6)	5 132(10)	−3 995(11)	−1 264(9)
C(7)	3 842(10)	−3 948(11)	−129(9)
C(8)	3 214(9)	−3 396(11)	−1 721(8)
C(9)	2 552(7)	−1 062(9)	−2 268(6)
C(10)	1 900(7)	−1 308(10)	−2 004(8)
C(11)	1 144(8)	−1 576(12)	−2 536(11)
C(12)	1 048(9)	−1 625(11)	−3 328(10)
C(13)	1 665(10)	−1 376(11)	−3 607(9)
C(14)	2 427(9)	−1 090(11)	−3 070(7)
C(15)	4 299(8)	−1 070(11)	−2 030(8)
C(16)	3 616(9)	552(10)	−1 550(8)

Data Collection and Processing.—Nicolet R3m diffractometer, ω-scan method ($2\theta \leqslant 100°$), graphite-monochomated Cu-K_α radiation. For (**1**), (**2**), (**4**), and (**5**) 2 050, 2 539, 2 489, and 2 364 independent measured reflections; 1 844, 2 359, 2 382, and 2 116 respectively considered observed [$|F_o| > 3\sigma(|F_o|)$], corrected for Lorentz and polarisation factors; analytical absorption corrections (face indexed crystals).

Structure Analysis and Refinement.—All four structures were solved by the heavy-atom method and the non-hydrogen atoms refined anisotropically. In (**2**), (**4**) and (**5**) the counter ions (PF_6^- and BF_4^-) were refined as rigid bodies. In these same structures the N–H hydrogen atom positions were determined from ΔF maps and these atoms were refined isotropically. In all cases the methyl groups were refined as rigid bodies. All other hydrogen atom positions were idealised (C–H 0.96 Å), assigned isotropic thermal parameters, $U(H) = 1.2U_{eq}(C)$, and allowed to ride on their parent carbons. In (**2**) a partial occupancy dichloromethane molecule was located from a ΔF map (site occupation factor 0.5) and this was subsequently refined anisotropically.

Refinement was by block-cascade full-matrix least-squares methods to give for (**1**) $R = 0.045$, $R' = 0.046$ [$w^{-1} = \sigma^2(F) + 0.000\,39F^2$], for (**2**) $R = 0.036$, $R' = 0.040$ [$w^{-1} = \sigma^2(F) + 0.000\,68F^2$], for (**4**) $R = 0.036$, $R' = 0.038$ [$w^{-1} = \sigma^2(F) +$

Table 2. Atomic co-ordinates ($\times 10^4$) for $[Pt(S_2N_2H)(PMe_2Ph)_2]Cl\cdot 0.5CH_2Cl_2$ (**2**)

Atom	*x*	*y*	*z*
Pt	−2 230(1)	371(1)	614(1)
S(1)	−1 106(3)	−765(1)	203(3)
S(2)	−2 248(3)	−10(1)	−1 490(2)
P(1)	−2 016(2)	723(1)	2 775(2)
P(2)	−3 420(2)	1 045(1)	−274(2)
N(1)	−1 387(8)	−307(3)	1 233(8)
N(2)	−1 604(8)	−592(3)	−1 245(8)
C(1)	−3 636(9)	884(3)	3 557(8)
C(2)	−3 900(10)	1 362(4)	4 139(9)
C(3)	−5 136(12)	1 470(5)	4 734(11)
C(4)	−6 164(12)	1 103(5)	4 758(12)
C(5)	−5 904(12)	623(5)	4 194(11)
C(6)	−4 676(11)	514(4)	3 574(11)
C(7)	−1 228(12)	286(4)	3 994(10)
C(8)	−917(10)	1 289(4)	2 984(11)
C(9)	−2 837(9)	1 686(3)	175(8)
C(10)	−3 562(10)	1 998(3)	1 061(10)
C(11)	−3 053(14)	2 459(4)	1 459(13)
C(12)	−1 794(16)	2 639(4)	950(13)
C(13)	−1 104(12)	2 341(4)	54(11)
C(14)	−1 604(10)	1 869(4)	−334(10)
C(15)	−3 488(13)	1 063(4)	−2 116(10)
C(16)	−5 214(10)	1 010(4)	173(12)
Cl(1)	−306(3)	−1 158(1)	3 304(3)
C(17)	2 074(22)	2 720(4)	2 082(28)
Cl(2)	2 073(11)	2 044(4)	2 109(14)
Cl(3)	3 475(12)	2 875(4)	3 143(10)

Table 3. Atomic co-ordinates ($\times 10^4$) for $[Pt(S_2N_2H)(PMe_2Ph)_2]PF_6$ (**4**)

Atom	*x*	*y*	*z*
Pt	2 229(1)	322(1)	−1 002(1)
S(1)	3 550(3)	−480(2)	755(1)
S(2)	2 529(3)	1 006(1)	220(1)
P(1)	2 057(3)	−445(1)	−2 175(1)
P(2)	1 213(2)	1 389(1)	−1 748(1)
P(3)	2 805(3)	−2 832(1)	302(1)
F(1)	4 073(5)	−2 240(3)	197(3)
F(2)	1 494(6)	−3 422(3)	379(4)
F(3)	1 510(5)	−2 232(3)	−98(4)
F(4)	4 050(6)	−3 433(3)	674(5)
F(5)	2 724(7)	−3 151(4)	−597(4)
F(6)	2 832(7)	−2 510(4)	1 174(3)
N(1)	3 075(9)	−593(4)	−236(4)
N(2)	3 250(11)	349(4)	964(4)
C(1)	120(10)	−511(5)	−2 836(5)
C(2)	−232(11)	−278(5)	−3 661(6)
C(3)	−1 761(13)	−291(7)	−4 154(8)
C(4)	−2 908(16)	−578(9)	−3 825(10)
C(5)	−2 571(13)	−833(7)	−3 002(11)
C(6)	−1 058(11)	−797(5)	−2 502(7)
C(7)	3 324(11)	−212(5)	−2 854(5)
C(8)	2 570(14)	−1 463(5)	−1 919(6)
C(9)	2 110(9)	1 633(4)	−2 589(5)
C(10)	3 693(10)	1 798(5)	−2 380(6)
C(11)	4 496(12)	1 944(6)	−2 997(7)
C(12)	3 676(14)	1 925(7)	−3 830(8)
C(13)	2 091(14)	1 786(7)	−4 042(6)
C(14)	1 326(9)	1 656(5)	−3 419(5)
C(15)	1 397(12)	2 270(5)	−1 140(6)
C(16)	−851(9)	1 320(5)	−2 210(6)

0.000 23F^2], and for (**5**) $R = 0.038$, $R' = 0.042$ [$w^{-1} = \sigma^2(F) + 0.000\,47F^2$]. The maximum residual electron densities in the final ΔF maps were 0.9, 1.2, 1.3, and 0.6 e Å^{-3} for (**1**), (**2**), (**4**), and (**5**) respectively. The mean and maximum shifts/error ratios in the final refinement cycle were 0.00 and 0.01 for (**1**), 0.01 and 0.06 for (**2**), 0.02 and 0.10 for (**4**), and 0.00 and 0.01 for (**5**). Inspection of the thermal parameters of N(1), S(1), N(2), and S(2) in (**1**) suggests a disorder phenomenon in this structure, whereby a proportion of the molecules in the crystal have adopted an orientation such that the positions of N(1) and S(2) and N(2) and S(1) are reversed. Unfortunately all attempts at refining a disordered model failed. This type of disorder has also been observed previously in the case of an iridium S_2N_2 complex.[10]

Table 4. Atomic co-ordinates ($\times 10^4$) for $[Pd(S_2N_2H)(PMe_2Ph)_2]BF_4$ (**5**)

Atom	*x*	*y*	*z*
Pd	1 865(1)	262(1)	−1 034(1)
S(1)	2 117(3)	−524(1)	759(1)
S(2)	2 814(3)	944(1)	213(1)
P(1)	833(2)	−500(1)	−2 242(1)
P(2)	2 273(2)	1 326(1)	−1 793(1)
N(1)	1 655(8)	−635(3)	−250(4)
N(2)	2 718(9)	307(4)	978(3)
C(1)	2 209(8)	−613(4)	−2 915(4)
C(2)	1 826(9)	−368(4)	−3 758(5)
C(3)	2 971(11)	−448(6)	−4 232(6)
C(4)	4 410(11)	−762(6)	−3 898(6)
C(5)	4 792(9)	−1 030(5)	−3 064(6)
C(6)	3 707(8)	−934(4)	−2 554(5)
C(7)	−1 090(8)	−221(4)	−2 939(4)
C(8)	447(11)	−1 499(4)	−1 973(5)
C(9)	540(7)	1 601(3)	−2 640(4)
C(10)	560(8)	1 604(4)	−3 496(4)
C(11)	−832(11)	1 778(5)	−4 120(5)
C(12)	−2 234(10)	1 945(5)	−3 900(5)
C(13)	−2 245(9)	1 963(4)	−3 057(5)
C(14)	−868(8)	1 783(4)	−2 428(4)
C(15)	3 967(8)	1 220(4)	−2 260(5)
C(16)	2 752(10)	2 212(4)	−1 162(5)
B(1)	2 297(5)	−2 698(2)	333(3)
F(1)	3 146(6)	−2 265(3)	−70(4)
F(2)	897(5)	−2 356(3)	291(3)
F(3)	3 102(7)	−2 777(5)	1 145(4)
F(4)	2 045(8)	−3 392(3)	−33(5)

Computations were carried out on an Eclipse S140 computer using the SHELXTL[11] program system and published[12] scattering factors.

Additional data available from the Cambridge Crystallographic Data Centre comprises thermal parameters, H-atom co-ordinates, and remaining bond parameters.

Results and Discussion

The atomic co-ordinates for complexes (**1**), (**2**), (**4**), and (**5**) are given in Tables 1—4 respectively. The crystal structures of (**1**) and (**4**) are shown in Figures 1 and 2 respectively. The bond lengths and angles together with those for related compounds are summarised in Tables 5 and 6. Comparison of the Pt–P(1) and Pt–P(2) bonds (*i.e.* phosphorus *trans* to sulphur and phosphorus *trans* to nitrogen) shows that in $[Pt(S_2N_2)(PMe_2Ph)_2]$ (**1**) and $[Pt(S_2N_2)(PMe_3)_2]$ (**8**)[8] there are no significant differences: 2.271(4), 2.265(3) Å for (**1**) and 2.268(5), 2.261(6) Å for (**8**). However in $[Pt(S_2N_2)(PPh_3)_2]$ (**6**)[4] a marked difference is observed with values of 2.317(4) and 2.263(5) Å respectively.* This difference is very similar to the effect observed in all the complexes containing the protonated ligand $S_2N_2H^-$, where the Pt–P(1) bond lengths are in the

* In a recent paper reporting the crystal structure of $[Pt(S_2N_2)(PPh_3)_2]\cdot C_6H_5CH_3$ similar Pt–P distances are reported.[13]

Table 5. Selected bond lengths (Å)

	Compound	M–P(1)	M–P(2)	M–S(2)	M–N(1)	N(1)–S(1)	S(1)–N(2)	N(2)–S(2)	Ref.*
(1)	$[Pt(S_2N_2)(PMe_2Ph)_2]$	2.271(4)	2.265(3)	2.270(5)	2.081(8)	1.466(10)	1.660(13)	1.560(14)	This work
(2)	$[Pt(S_2N_2H)(PMe_2Ph)_2]Cl$	2.314(2)	2.261(2)	2.286(2)	2.025(7)	1.582(8)	1.561(8)	1.647(8)	This work
(3)	$[Pt(S_2N_2H)(PMe_2Ph)_2]BF_4$	2.303(2)	2.261(2)	2.283(2)	2.015(7)	1.595(7)	1.538(9)	1.649(8)	1
(4)	$[Pt(S_2N_2H)(PMe_2Ph)_2]PF_6$	2.305(2)	2.262(2)	2.282(2)	2.038(7)	1.589(7)	1.501(8)	1.670(8)	This work
(5)	$[Pd(S_2N_2H)(PMe_2Ph)_2]BF_4$	2.326(2)	2.276(2)	2.290(2)	2.031(6)	1.588(6)	1.527(7)	1.668(7)	This work
(6)	$[Pt(S_2N_2)(PPh_3)_2]$	2.317(4)	2.263(5)	2.288(5)	2.019(14)	1.546(16)	1.567(19)	1.681(16)	4
(7)	$[\{Pt(S_2N_2)(PPh_3)\}_2]$		2.255(4)	2.219(4)	2.042(12)	1.552(12)	1.528(13)	1.687(14)	5
(8)	$[Pt(S_2N_2)(PMe_3)_2]$	2.268(5)	2.261(6)	2.268(6)	2.085(14)	1.492(13)	1.576(16)	1.668(17)	8
(9)	$[Pt(S_2N_2)(PPh_3)_2]$	2.308(5)	2.259(3)	2.294(6)	2.093(13)	1.499(16)	1.702(15)	1.548(12)	13
(10)	$[Pt(S_2N_2H)(PEt_3)_2][SnMe_2Cl_3]$	2.306(4)	2.263(3)	2.281(4)	2.091(9)	1.572(12)	1.554(10)	1.667(10)	9
(11)	$[\{Pt(S_2N_2H)(PBu^n_3)_2\}_2]Cl[PF_6]$	2.311(2)	2.262(2)	2.291(2)	2.024(6)	1.585(5)	1.544(8)	1.662(8)	9
		2.318(2)	2.273(2)	2.277(2)	2.034(6)	1.590(7)	1.543(7)	1.650(7)	9

* All literature numbering schemes transposed to those for **(1)**, **(2)**, **(4)**, and **(5)**.

Table 6. Selected bond angles (°)

Compound	P(1)–M–P(2)	P(1)–M–N(1)	P(2)–M–S(2)	N(1)–M–S(2)	M–N(1)–S(1)	N(1)–S(1)–N(2)	S(1)–N(2)–S(2)	N(2)–S(2)–M	Ref.
(1)	94.4(1)	88.7(3)	92.0(1)	85.0(3)	117.3(6)	113.8(6)	116.0(9)	107.4(5)	This work
(2)	95.1(1)	92.0(2)	89.2(1)	84.1(2)	121.9(5)	108.2(4)	120.5(5)	105.3(3)	This work
(3)	94.3(1)	90.9(2)	90.3(1)	84.6(2)	121.4(4)	108.1(4)	121.6(5)	104.4(3)	1
(4)	94.2(1)	90.8(2)	90.3(1)	84.7(2)	120.2(4)	109.4(4)	122.1(5)	103.7(3)	This work
(5)	94.4(1)	91.2(2)	89.7(1)	84.7(2)	120.7(3)	109.2(3)	121.3(4)	104.0(2)	This work
(6)	98.4(2)	82.8(5)	91.1(2)	87.7(5)	116.1(9)	116.1(9)	116.2(11)	104.0(7)	4
(7)			94.8(1)	88.0(3)	116.3(6)	112.7(7)	119.7(8)	103.1(4)	5
(8)	98.0(3)	84.2(5)	91.5(3)	86.4(5)	115.3(8)	117.7(8)	115.0(8)	105.5(6)	8
(9)	97.8(1)	84.8(4)	90.8(1)	86.8(4)	113.5(7)	117.5(7)	113.7(8)	108.4(7)	13
(10)	97.9(1)	87.0(3)	90.8(1)	84.3(3)	121.2(6)	109.4(5)	119.8(7)	105.2(4)	9
(11)	98.4(1)	86.1(1)	91.0(1)	84.5(1)	121.1(3)	109.3(3)	120.4(4)	104.7(3)	9
	99.0(1)	87.2(2)	89.4(1)	84.4(2)	120.8(4)	108.8(4)	120.7(4)	105.2(3)	9

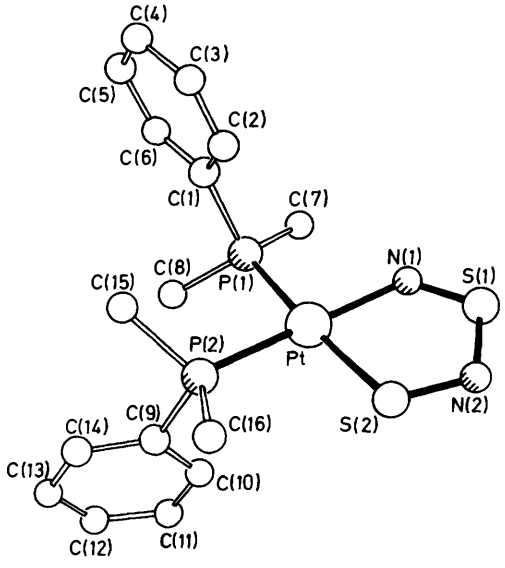

Figure 1. The crystal structure of the molecule in $[Pt(S_2N_2)(PMe_2Ph)_2]$ **(1)**

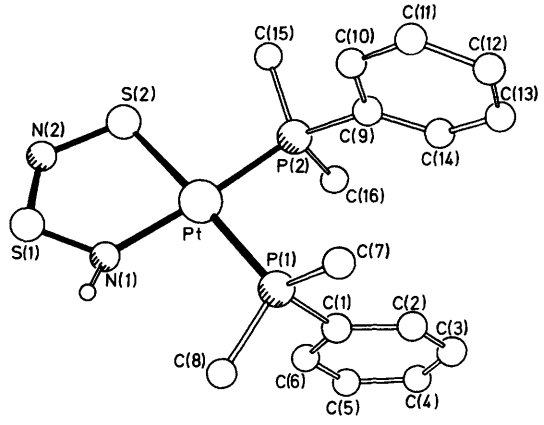

Figure 2. The crystal structure of the cation in $[Pt(S_2N_2H)(PMe_2Ph)_2]PF_6$ **(4)**

range 2.303(2)—2.318(2) Å and those for Pt–P(2) in the range 2.261(2)—2.273(2) Å. Thus, the effect of protonation of the nitrogen on the $S_2N_2^{2-}$ ligand is to lengthen the Pt–P bond *trans* to sulphur whilst that *trans* to the nitrogen is not significantly affected. $^{31}P-\{^1H\}$ N.m.r. studies[9] on the $S_2N_2^{2-}$ and $S_2N_2H^-$ complexes reveal that upon protonation the magnitude of $J(^{195}Pt-^{31}P)$ decreases for P(1) (*trans* to sulphur) in accord with the increase in bond length. The coupling for P(2) (*trans* to nitrogen) increases although the Pt–P bond lengths are unchanged. This reflects the difference in *trans* influence of the imine and imide nitrogens in the two types of complex.

The Pt–S bond lengths are nearly all similar [2.268(6)—2.294(6) Å], the only exception being the binuclear complex (**7**)[5] at 2.219(4) Å. In this latter case the difference almost certainly reflects the presence of a nitrogen atom *trans* to the sulphur, *cf.* phosphorus in all the other complexes.

The Pt–N bond lengths do not show any variation on protonation.

Equivalent S–N bonds show considerable variation for the non-protonated complexes but are generally more consistent for the $S_2N_2H^-$ ligand. In the protonated species, the N(1)–S(1) bond lengths lie in the range 1.572(12)—1.595(7) Å, S(1)–N(2)

Table 7. Stacking characteristics and intercation separations (Å) in selected $S_2N_2H^-$ complexes

Compound	Ref.	Type of stacking	Intradimer interplanar separation	Intradimer closest contact	Interdimer interplanar separation	Interdimer closest contact
(2)	This work	Stacked dimers	3.48	3.50 Pt–S(1)	5.40	5.52 Pt–S(2)
(3)	1	Stacked dimers	3.53	3.62 Pt–S(1)	4.67	4.70 Pt–N(2)
(4)	This work	Stacked dimers	3.58	3.67 Pt–S(1)	5.00	5.00 Pt–N(2)
(5)	This work	Stacked dimers	3.50	3.50 Pd–S(1)	4.69	4.73 Pd–N(2)
(11)	9	Isolated dimers (for one of the two independent molecules)	3.63	3.66 S(1)–S(2)		

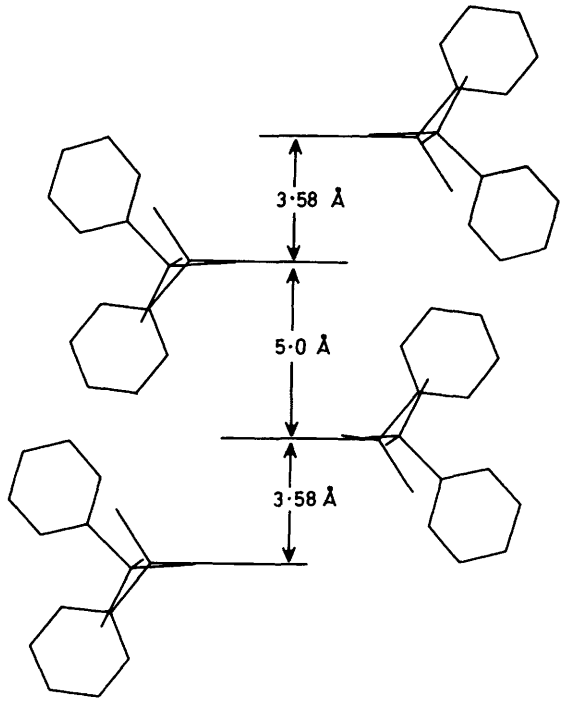

Figure 3. A view perpendicular to the normal of the mean plane of the PtS_2N_2 ring of a pair of dimers in $[Pt(S_2N_2H)(PMe_2Ph)_2]PF_6$ (**4**) showing the alternating long and short contacts

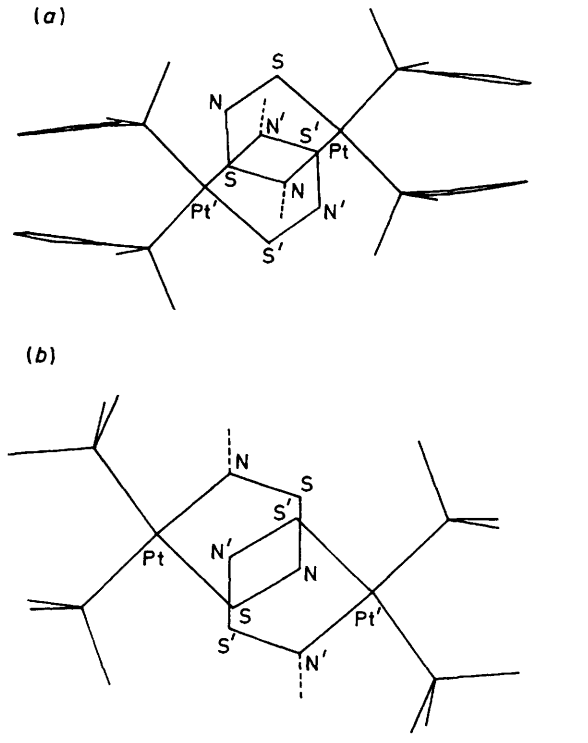

Figure 4. A dimer pair in (*a*) $[Pt(S_2N_2H)(PMe_2Ph)_2]PF_6$ (**4**) and (*b*) $[\{Pt(S_2N_2H)(PBu^n_3)_2\}_2]Cl[PF_6]$ (**11**) viewed perpendicular to the mean plane of the PtS_2N_2 ring

in the range 1.501(8)—1.561(8) Å, and N(2)—S(2) in the range 1.647(8)—1.670(8) Å. Structures (**2**), (**3**), and (**4**) appear to show a trend whereby there is a decrease in the S(1)–N(2) bond length as the size of the counter ion increases ($Cl^- \longrightarrow PF_6^-$). Coincident with this (Table 7) the interplanar separations of the overlapping PtS_2N_2 regions of the cations increase, which may be explained as follows. Since, in all instances, there is cation–anion hydrogen bonding through N(1)–H, one limiting factor in the close approach of the cations will be the electrostatic repulsion between anions which depends, in part, on the size of the anion.

The variation of the S(1)–N(2) distance with counter ion/interplanar separation merits further discussion. The largest intercation separation, in $[Pt(S_2N_2H)(PMe_2Ph)_2]PF_6$ (**4**), is associated with the shortest S(1)–N(2) bond. The S(1)–N(2) bond has substantial π character and there is a low-lying empty π^* orbital associated with the $S_2N_2H^-$ ligand. Hence it is possible to speculate that on the close approach between Pt and S(1) of adjacent cations electron density is transferred from the platinum d_{z^2} orbital into an orbital which is antibonding with respect to S(1)–N(2). Thus the closer the cations, the longer the S(1)–N(2) bond length.

Interpretation of the S–N bond lengths for the $S_2N_2^{2-}$ complexes is much more difficult due to the notably greater range of values. The bond lengths for (**1**) should be discounted as this structure is partially disordered (see Experimental section) and therefore the bond lengths for the PtS_2N_2 ring will be shifted from their true values. The only structure so far reported whose bond lengths are in agreement with those for (**1**) is (**9**).[13] However in (**9**) we suspect, from inspection of the relative sizes of the published thermal ellipsoids, a similar disorder phenomenon to that described here for (**1**). Additional support for this conclusion arises from an analysis of the analogous complex $[Pt(S_2N_2)(PPh_3)_2]\cdot 4CHCl_3$ (**6**). With the exception of the two disordered structures, (**1**) and (**9**), the remaining neutral species, (**6**) and (**8**), show fair internal agreement (Table 5). The binuclear compound (**7**) shows bond lengths which do not differ significantly from the values for (**6**) and (**8**), although other workers (using very limited data) have claimed the contrary.[14]

The bond angles (Table 6) around the metallacycle show very clearly the marked effect of protonation of the $S_2N_2^{2-}$ ligand. For the neutral complexes the angles M–N(1)–S(1),

N(1)–S(1)–N(2), S(1)–N(2)–S(2), and N(2)–S(2)–M occur in the ranges 115.3(8)—116.3(6), 112.7(7)—117.7(8), 115.0(8)—119.7(8), and 103.1(4)—105.5(6)° respectively [excluding (**1**) and (**9**) for the reasons given above]. For the protonated species the equivalent values are 120.2(4)—121.9(5), 108.1(4)—109.4(5), 119.8(7)—122.1(5), and 103.7(3)—105.3(3)°. Thus when protonated N(1) assumes an sp^2 trigonal geometry rather than the intermediate geometry in the neutral case. The angle at S(1) closes from an intermediate sp^2/sp^3 to a tetrahedral sp^3 angle on protonation. N(2) behaves in a very similar manner to N(1) in going to a trigonal geometry. There is no alteration at S(2).

The effect of protonation on the S–N portion of the metallacycle may be broadly summarised as (*i*) an increase in N(1)–S(1), (*ii*) a decrease in S(1)–N(2), (*iii*) no significant change in N(2)–S(2), (*iv*) a change from intermediate to trigonal geometry at both nitrogens, and (*v*) a decrease in the angle at S(1).

Thus it appears that the most significant diagnostic test for the presence of the hydrogen atom on N(1) is the value of the angles at N(1) and N(2).

In the majority of the ionic compounds a characteristic stacking arrangement of the $M(S_2N_2H)$ rings is observed, Figure 3. Table 7 summarises relevant inter-ring contacts. The only cation studied which does not form stacks or isolated dimer pairs is in (**10**) where the bulky anion ($[SnMe_2Cl_3]^-$), to which the cation is hydrogen bonded, prevents this.

In (**11**) the cations form isolated dimer pairs. This is due to the extremely bulky nature of the PBu^n_3 ligands which can arrange themselves so as to allow the close approach of one other cation but in so doing block any approach of the second cation from the other side. The resulting interplanar separation within this dimer of 3.63 Å is very similar to that for the other compound, (**4**), containing a PF_6^- counter ion, where the separation is 3.58 Å. Complex (**11**) is also distinguished by the degree of ring overlap [Figure 4(*b*)] which is considerably less than in any of the other compounds and results in the closest intradimer atomic contact being 3.66 Å between S(1) and S(2′). In the other structure it is S(1)—M′ which is the shortest contact.

Compounds (**3**), (**4**), and (**5**) all display stacking that is very similar, both within the dimer unit and between separate dimer pairs. The contacts in (**4**) are slightly lengthened due to the bulky PF_6^- counter ion but the overlap is otherwise similar. Complex (**2**) however behaves differently from (**3**), (**4**), and (**5**) in that although it has the least bulky anion [and consequently the shortest intradimer contacts, 3.50 Å for Pt–S(1′)], it has interdimer pair separations which are even larger than for the PF_6^- case in (**4**) (5.40 Å compared with 5.00 Å). The close similarity between (**3**) and (**5**) shows that substituting Pd for Pt has no significant effect on the stacking.

In assessing the probable mode of stacking (or dimer formation) two factors are important: (*a*) the bulkiness of the phosphine, although having little effect on intradimer separations, does significantly perturb the interdimer arrangement and (*b*) the bulk of the anion is critical and can in some instances totally disrupt the structural arrangement.

Acknowledgements

We are grateful to Johnson Matthey Ltd. for the loan of precious metals.

References

1 R. Jones, P. F. Kelly, C. P. Warrens, D. J. Williams, and J. D. Woollins, *J. Chem. Soc., Chem. Commun.*, 1986, 711.
2 N. P. C. Walker, M. B. Hursthouse, C. P. Warrens, and J. D. Woollins, *J. Chem. Soc., Chem. Commun.*, 1985, 227.
3 J. D. Woollins, *Polyhedron*, 1984, **3**, 1365.
4 R. Jones, P. F. Kelly, D. J. Williams, and J. D. Woollins, *Polyhedron*, 1985, **4**, 1947.
5 R. Jones, P. F. Kelly, D. J. Williams, and J. D. Woollins, *J. Chem. Soc., Chem. Commun.*, 1985, 1325.
6 J. D. Woollins, R. Grinter, M. K. Johnson, and A. J. Thomson, *J. Chem. Soc., Dalton Trans.*, 1980, 1910.
7 P. F. Kelly and J. D. Woollins, *Polyhedron*, 1986, **5**, 607.
8 P. A. Bates, M. B. Hursthouse, P. F. Kelly, and J. D. Woollins, *J. Chem. Soc., Dalton Trans.*, 1986, 2367.
9 R. Jones, C. P. Warrens, D. J. Williams, and J. D. Woollins, *J. Chem. Soc., Dalton Trans.*, 1987, 907.
10 F. Cecconi, C. A. Ghilardi, S. Midollini, S. Moneti, and A. Orlandini, *J. Organomet. Chem.*, 1984, **275**, C22.
11 G. M. Sheldrick, SHELXTL, An integrated system for solving, refining, and displaying crystal structures from diffraction data, University of Göttingen, Federal Republic of Germany, 1978; Revision 4.1, 1983.
12 'International Tables for *X*-Ray Crystallography,' Kynoch Press, Birmingham, 1974, vol. 4, pp. 99—149.
13 T. Chivers, F. Edelmann, U. Behrens, and R. Drews, *Inorg. Chim. Acta*, 1986, **116**, 145.
14 C. A. Ghilardi, S. Midollini, S. Moneti, and A. Orlandini, *J. Organomet. Chem.*, 1985, **286**, 419.

Received 18*th February* 1987; *Paper* 7/299